



# Assessment of photosynthetic activity in dense microalgae cultures using oxygen production

Antoni Mateu Vera-Vives, Tim Michelberger, Tomas Morosinotto, Giorgio Perin \*

Department of Biology, University of Padova, 35131, Padova, Italy

## ARTICLE INFO

Handling Editor: Dr. Mario De Tullio

### Keywords:

Microalgae  
*Nannochloropsis*  
 Oxygen evolution  
 Photosynthesis  
 Genetic engineering  
 Photobioreactor

## ABSTRACT

Microalgae are photosynthetic microorganisms playing a pivotal role in primary production in aquatic ecosystems, sustaining the entry of carbon in the biosphere. Microalgae have also been recognized as sustainable source of biomass to complement crops. For this objective they are cultivated in photobioreactors or ponds at high cell density to maximize biomass productivity and lower the cost of downstream processes.

Photosynthesis depends on light availability, that is often not constant over time. In nature, sunlight fluctuates over diurnal cycles and weather conditions. In high-density microalgae cultures of photobioreactors outdoors, on top of natural variations, microalgae are subjected to further complexity in light exposure. Because of the high-density cells experience self-shading effects that heavily limit light availability in most of the mass culture volume. This limitation strongly affects biomass productivity of industrial microalgae cultivation plants with important implications on economic feasibility.

Understanding how photosynthesis responds to cell density is informative to assess functionality in the inhomogeneous light environment of industrial photobioreactors. In this work we exploited a high-sensitivity Clark electrode to measure microalgae photosynthesis and compare cultures with different densities, using *Nannochloropsis* as model organism. We observed that cell density has a substantial impact on photosynthetic activity, and demonstrated the reduction of the cell's light-absorption capacity by genetic modification is a valuable strategy to increase photosynthetic functionality on a chlorophyll-basis of dense microalgae cultures.

## 1. Introduction

Photosynthetic organisms are responsible for primary production, sustaining most lifeforms on our planet (Cavicchioli et al., 2019). Among them, eukaryotic microalgae are unicellular species that play a pivotal role in the biosphere, being responsible for approx. 50% of global primary production (Kirchman, 2018). Thousands of different microalgae species exist (Guiry, 2012), as the result of evolution in many ecological niches, where they are often placed at the basis of the existing food web, representing the primary producers and thus the main responsible of organization of atmospheric carbon.

Beside their fundamental ecological role, microalgae are also gaining increasing interest as bio-factories to convert the current fossil-fuels-based economy to a bio-based solar-driven alternative, for a more sustainable future (Olabi et al., 2023). Microalgae have a higher maximum photosynthetic rate than plants on a whole-organism dry-weight basis when cultivated in optimal conditions (i.e. non-limiting supply of nutrients and CO<sub>2</sub>) (Heaton et al., 2008; Weyer et al., 2010; Zhu et al.,

2008), mainly because their whole organism is photosynthetically active, at difference from terrestrial plants that have non-photosynthetic tissues. This leads to higher rates of CO<sub>2</sub> and nutrients sequestration, enabling their cultivation in strict connection to industrial and civil sites to mitigate greenhouse gases emissions and water pollution (Ma et al., 2022; Molazadeh et al., 2019; Perin et al., 2019). Moreover, their huge metabolic plasticity, developed in thousands of years of evolution in different ecological niches shaped the ability to accumulate a plethora of metabolites finding many applications in the current economy, e.g. from biofuels to food additives (Khan et al., 2018; Perin and Morosinotto, 2019a).

In microalgae, as in many other photosynthetic eukaryotes, the homeostasis of the central metabolism depends on the energetic and redox status of the cell, which is balanced by the activity of two organelles, i.e. chloroplasts and mitochondria. In many microalgae species mitochondrial respiration shows a minimal activity (10–15% of gross photosynthetic rate) and only sustains cell maintenance (Formighieri et al., 2012; Masojidek et al., 2021). On the other hand, in strictly photoautotrophic

\* Corresponding author.

E-mail address: [giorgio.perin@unipd.it](mailto:giorgio.perin@unipd.it) (G. Perin).

microalgae species the photosynthetic activity of the chloroplast is the final source of energy to sustain the central metabolism.

Chloroplasts contain membrane-bound enzymatic complexes that mediate photosynthesis, driving both i) the transfer of electrons from a reduced substrate (i.e. water) to an oxidized product (i.e. NADP<sup>+</sup>) and ii) the translocation of protons across a biological membrane to generate a proton motive force that fuels the synthesis of chemical energy in form of ATP by the action of ATP synthase.

Photosynthetic activity in the chloroplast depends on the availability of light energy, which in nature changes over diurnal cycles and weather conditions, affecting photosynthetic functionality and consequently microalgae fitness. The ability to respond to environmental changes in light availability is one of the phenomena at the base of the success of some microalgae species over others in different ecological niches, with implications for the functionality of the very ecosystem (Morgan-Kiss et al., 2006).

On the other hand, when microalgae biomass is to be exploited for industrial applications, these organisms are cultivated in open or closed systems, i.e. ponds or photobioreactors (PBRs), respectively, that operate with high cell density to maximize biomass productivity (Ruiz et al., 2016). In such conditions, the high density leads to cell's self-shading and prevents light to homogeneously reach all the regions of the mass culture, generating a light gradient from external to internal regions (Formighieri et al., 2012; Perin and Morosinotto, 2019b; Schediwiy et al., 2019). External regions receive excess light and internal regions limiting irradiance, curbing global light-use efficiency in photobioreactors. Microalgae cultures at industrial scale are also actively mixed to i) increase the average exposition of the mass culture to light and ii) optimize the supply of both nutrients and CO<sub>2</sub> (de Souza Kirnev et al., 2022). Because of mixing, microalgae are constantly moved from most-exposed to light-limited regions of the culture (and *viceversa*) and experience fast fluctuations of irradiance to which regulatory mechanisms of photosynthesis are only partially able to respond to, affecting light-use efficiency and biomass productivity in photobioreactors (Bellan et al., 2020; Perin and Morosinotto, 2023). The impact of this complex light environment on microalgae physiology is still under-investigated (Masojídek et al., 2021), which is one of the most relevant causes for the limited success of the optimization efforts of microalgae cultivation at scale so far (Perin et al., 2022).

A more systematic investigation of how photosynthesis responds in high-density cultures, focusing e.g. on the influence of phenomena such as self-shading, is an unavoidable task to understand how microalgae deal with the complex environmental light conditions of photobioreactors and ultimately to deploy effective optimization efforts.

In this work, we used a high-sensitivity Clark electrode to measure the photosynthesis-irradiance relationship of microalgae cultures with different densities, using *Nannochloropsis gaditana* as experimental model. We quantified the impact of cell density on microalgae photosynthetic activity, showing how self-shading plays a relevant role in dense cultures. This hypothesis was validated by using as tools pale mutants accumulating less chlorophyll (Chl) per cell, which demonstrated that the larger the reduction in pigment content, the higher is the increase in photosynthetic activity on a Chl-basis.

## 2. Materials and methods

### 2.1. Microalgae strains and culture conditions

#### 2.1.1. Strains

In this work we used the microalgal species *Nannochloropsis gaditana*, strain CCAP 849/5, that was purchased from the Culture Collection of Algae and Protozoa (CCAP).

#### 2.1.2. Culture conditions

*N. gaditana* was maintained in F/2 solid medium, following the original recipe (Guillard and Ryther, 1962), containing 32 g l<sup>-1</sup> sea salts

(Sigma Aldrich), 40 mM Tris-HCl pH 8, Guillard's (F/2) marine water enrichment solution (Sigma Aldrich) and 1% agar (Duchefa Biochemie).

Cells were pre-cultured in sterile F/2 liquid media in Erlenmeyer flasks and in plastic flasks with ventilation caps exposed at 100 μmol of photons m<sup>-2</sup> s<sup>-1</sup> with 100 rpm agitation, at 22 ± 1 °C in a growth chamber. Growth curves were performed in the same conditions of pre-cultures from cells washed twice in fresh F/2 media, starting from 5·10<sup>6</sup> cells ml<sup>-1</sup> concentration in sterile F/2 liquid media supplemented with 10 mM NaHCO<sub>3</sub> to avoid carbon limitation.

### 2.2. Preparation of cells for measurements of oxygen evolution

Cell concentration was measured with an automatic cell counter (Cellometer Auto X4, Cell Counter, Nexcelom) at the fourth day of cultivation in the growth conditions described above. Cells were collected via mild centrifugation at 3500 g for 10 min at room temperature and then resuspended in fresh sterile F/2 media supplemented with 10 mM NaHCO<sub>3</sub> right before the start of the oxygen evolution assessment, which did not last longer than 1 h, to avoid both nutrients and carbon limitation during the measurement.

### 2.3. High resolution oxygen evolution

Oxygen evolution was measured at the fourth day of the growth curves described above. Measurements were performed using a test version of the NextGen-O2k and the PhotoBiology (PB)-Module (Oroboros Instruments, Innsbruck) with the software DatLab 7.4.0.4 (Went et al., 2021), according to the methods developed in (Vera-Vives et al., 2022). The PB light source contained a blue OSLO® LED (emitting wavelength range 439–457 nm with the peak at 451 nm, manufactured by OSRAM) attached to the window of the NextGen-O2k chamber.

The oxygen concentration was assessed in 2-ml measuring chambers (cylindrical chambers with 1 cm diameter x 2 cm height) at 22 °C with a frequency of 2 s<sup>-1</sup> and samples were magnetically stirred at 750 rpm (12.5 Hz). This is the maximum mixing speed recommended by the manufacturer to achieve an optimal O<sub>2</sub> diffusion indeed (Gnaiger, 2001; "MiPNet22.11 O2k-FluoRespirometer manual - Bioblast," n.d.), as confirmed by other works using the same instrument also with different microalgae species (Went et al., 2021).

Two measurements were performed in parallel at each time, taking advantage of the two chambers of the instrument.

At first, the measuring chambers were filled with fresh and sterile F/2 medium, containing 10 mM NaHCO<sub>3</sub> to avoid carbon limitation during the measurement and to equilibrate the temperature at 22 °C for few minutes. Then, a fraction of the medium (<10% of the chamber volume) was replaced with a suspension of *Nannochloropsis* cells to reach the desired final concentration in the measuring chamber. The chambers were then closed, and the samples were dark adapted (at least for 10 min until the oxygen consumption rate was constant) to assess the respiration rate before starting the measurements of the rate of oxygen evolution at increasing irradiances.

After stabilization of the respiration signal, light was turned on at increasing irradiances, waiting at least 5 min at each light intensity to achieve the stabilization of the oxygen evolution rate (on average the trace indicating the rate of oxygen evolution stabilized within the first 2–3 min, Supplementary Fig. S1). The values of oxygen evolution rate reported in this work at each irradiance correspond to the median of 40–50 points in the stable region of the rate of oxygen evolution.

Respiration and photosynthesis rates at different irradiances were calculated with the software DatLab 7.4.0.4. It is worth noting that the photosynthetic parameters extrapolated from the photosynthesis-irradiance curves were not influenced by the starting concentration of molecular oxygen, as a preliminary equilibration phase of the measuring medium in presence of atmospheric oxygen was carried out for all tested samples.

## 2.4. Determination of chlorophyll content

After evaluation of oxygen evolution, microalgae samples were further processed to extract chlorophyll molecules from *Nannochloropsis* cells, using 1:1 ratio of 100% N, N-dimethylformamide (DMF) (Sigma Aldrich), at 4 °C in the dark, for at least 24 h (Wellburn, 1994). The chlorophyll concentration was calculated, using specific extinction coefficients (Wellburn, 1994), from the absorption values at 664 nm of DMF *Nannochloropsis* extracts, collected using a Cary 100 spectrophotometer (Agilent Technologies).

## 2.5. Statistical analysis

In this work, we performed a statistical hypothesis testing for all the data presented. Statistical significance was assessed by *t*-test using OriginPro 2020 (v. 9.7.0.188) (<http://www.originlab.com/>). Samples size was at least 4 for all the measurements collected in this work. Data were fitted with the equation defined in (Ye, 2007), using a minimum mean square error-based approach using OriginPro 2020 (v. 9.7.0.188).

## 3. Results

### 3.1. Estimation of photosynthetic functionality from oxygen evolution

*Nannochloropsis* cells grown in lab-scale cultures, as described in the materials and methods section, were used to investigate the photosynthesis-irradiance (PI) relationship of samples with increasing cell concentration. Fig. 1 shows data obtained with  $5 \cdot 10^6$  cells  $\text{ml}^{-1}$ , corresponding to a Chl concentration of  $4 \mu\text{g Chl ml}^{-1}$ . Lower concentrations (down to  $1 \cdot 10^6$  cells  $\text{ml}^{-1}$ ) have a higher noise but still were able to generate traces of sufficient quality for a reliable extrapolation of the parameters describing the photosynthetic activity of *Nannochloropsis* cells (Supplementary Fig. S2).

*Nannochloropsis* samples at a concentration of  $5 \cdot 10^6$  cells  $\text{ml}^{-1}$  showed a dark respiration rate ( $R_D$ ) of  $1.31 \pm 0.12$   $\text{pmol O}_2 \text{ s}^{-1} \cdot 10^{-6}$  cells. Light intensity was then progressively increased from 0 to 200  $\mu\text{mol photons s}^{-1} \text{ m}^{-2}$ . The light compensation point (i.e.  $I_{\text{comp}}$ , namely the irradiance value where the dark respiration is fully compensated by the photosynthetic activity rate) was  $12.2 \pm 1.1$   $\mu\text{mol photons s}^{-1} \text{ m}^{-2}$ , while the saturation threshold (i.e.  $I_{\text{sat}}$ , namely the irradiance value at which the photosynthetic rate does not increase with irradiance any longer) was  $163 \pm 27$   $\mu\text{mol photons s}^{-1} \text{ m}^{-2}$ . The maximal gross photosynthetic rate was instead  $4.6 \pm 0.2$   $\text{pmol O}_2 \text{ s}^{-1} \cdot 10^{-6}$  cells.

In this work we exploited a high-sensitivity Clark electrode (i.e. NextGen-O2k) for quantifying photosynthesis which enables higher resolution compared to alternative versions. The NextGen-O2k has a resolution of 2 nM and the limit of detection of the rate of oxygen evolution is  $0.001 \mu\text{M s}^{-1}$  (Doerrier et al., 2018; Gnaiger, 2008), therefore enabling the reliable detection of small differences in  $\text{O}_2$  concentration. It is in fact worth noting that we could decrease the cell concentration by a 30x factor, compared to similar experiments with an alternative Clark-type sensor (Perin et al., 2015). Consequently, we could determine the photosynthetic parameters above detailed with relatively low-concentration microalgae samples, without sacrificing the reproducibility. The minimization of the volume of the microalgae culture has a twofold important implication: i) self-shading effects during the measurements are minimized for an unbiased determination of photosynthetic parameters and ii) changes in the rate of oxygen evolution per volume of culture are relatively small, enabling to run even longer-time experiments without reaching saturation with possible negative effects on microalgae cells.

### 3.2. Dependence of photosynthetic functionality on cell concentration

Thanks to the instrumentation sensitivity it was even possible to assess the impact of self-shading by measuring samples of

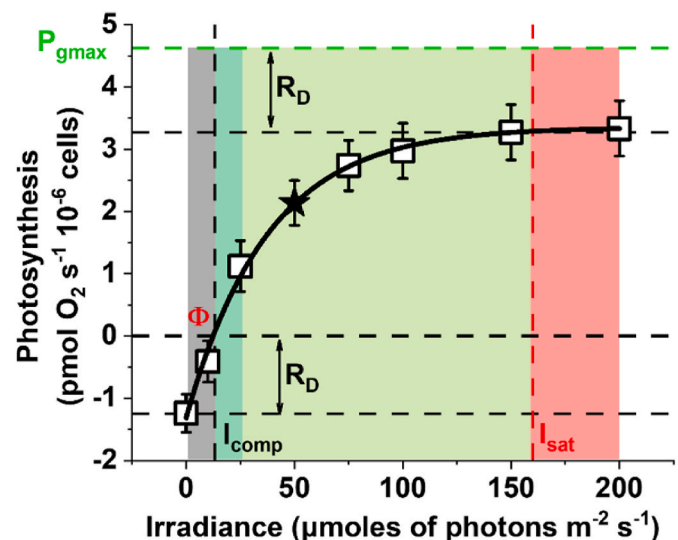


**Fig. 1. Dependence of Photosynthesis on light intensity.** Data shown here were assessed from a *Nannochloropsis* culture with  $5 \cdot 10^6$  cells  $\text{ml}^{-1}$  cells concentration, corresponding to  $4 \mu\text{g Chl ml}^{-1}$ . Photosynthesis is expressed as rate of  $\text{O}_2$  evolution and it is normalized to the number of cells. Light intensity is expressed as irradiance.  $I_{\text{comp}}$  and  $I_{\text{sat}}$  indicate the light compensation and light saturation points, respectively, both expressed as  $[\mu\text{mol photons s}^{-1} \cdot \text{m}^{-2}]$ .  $R_D$  is the dark  $\text{O}_2$  respiration rate, expressed as  $[\text{pmol} \cdot \text{s}^{-1} \cdot 10^{-6}$  cells].  $P_{\text{gmax}}$  is the maximal gross  $\text{O}_2$  photosynthetic rate, expressed as  $[\text{pmol} \cdot \text{s}^{-1} \cdot 10^{-6}$  cells].  $\Phi_{(I_0 - I_{\text{comp}})}$  is the quantum yield in the range between  $I_0$  and  $I_{\text{comp}}$   $[\text{pmol O}_2 \cdot \text{m}^2 \cdot \mu\text{mol photons}^{-1} \cdot 10^{-6}$  cells]. The black star indicates the photosynthetic activity (expressed as rate of  $\text{O}_2$  evolution) at  $50 \mu\text{mol photons s}^{-1} \text{ m}^{-2}$ , a parameter used in the following analysis. In this scheme, four irradiance regions have been highlighted with different colors, according to their relationship with the photosynthetic rate: grey, from dark to  $I_{\text{comp}}$  where the respiration rate is higher than the photosynthetic rate; dark green, region of light limitation, from  $I_{\text{comp}}$  to the end of the linearity range, where the photosynthetic rate linearly increases with irradiance (Pearson's  $r = 0.99$ ), described by the equation:  $y = (-1.3 \pm 0.07) + (0.09 \pm 0.005)x$  with a slope significantly different from 0 (Test-t,  $p$ -value  $< 0.05$ ); light green, from the end of the linearity range to  $I_{\text{sat}}$  where the photosynthetic rate doesn't linearly increase with irradiance and cells are no longer limited by light; red, irradiances beyond  $I_{\text{sat}}$  where the photosynthetic rate no longer increases with irradiance. Every point in this figure represents the average value of 4 biological replicates  $\pm$  SD. The data for each biological replicate at each irradiance come from the median value of 40 datapoints where the  $\text{O}_2$  evolution trace was more stable (Supplementary Fig. S1).

*Nannochloropsis* with increasing cell concentrations, from  $2.5 \cdot 10^6$  cells  $\text{ml}^{-1}$  to  $100 \cdot 10^6$  cells  $\text{ml}^{-1}$  (Fig. 2). For a fair comparison, we used the photosynthetic activity data collected at  $50 \mu\text{mol photons m}^{-2} \text{ s}^{-1}$ , namely an irradiance value neither limiting nor saturating for photosynthesis (black star in Fig. 1).

All cells were exposed to the same light conditions during cultivation ensuring an identical acclimation state (average Chl content of  $0.08 \mu\text{g Chl} \cdot 10^{-6}$  cells).

From  $2.5 \cdot 10^6$  cells  $\text{ml}^{-1}$  to  $20 \cdot 10^6$  cells  $\text{ml}^{-1}$  samples showed a constant rate of  $\text{O}_2$  evolution, whilst the latter decreased as the cell concentration increased up to the highest concentration tested in this work ( $100 \cdot 10^6$  cells  $\text{ml}^{-1}$ , Fig. 2). Overall, cell concentrations could be divided into two groups according to the behavior observed in Fig. 2: i) for samples between  $2.5 \cdot 10^6$  cells  $\text{ml}^{-1}$  and  $20 \cdot 10^6$  cells  $\text{ml}^{-1}$  there was no significant difference between the measured photosynthetic activity, suggesting that in this range data are not influenced by the cell concentration and thus the self-shading effects during the measurements are negligible. In the former case, with  $2.5 \cdot 10^6$  cells  $\text{ml}^{-1}$ , the noise of the measurements was higher because of the low cell concentration. ii) for samples in the range between  $20 \cdot 10^6$  cells  $\text{ml}^{-1}$  and  $100 \cdot 10^6$  cells

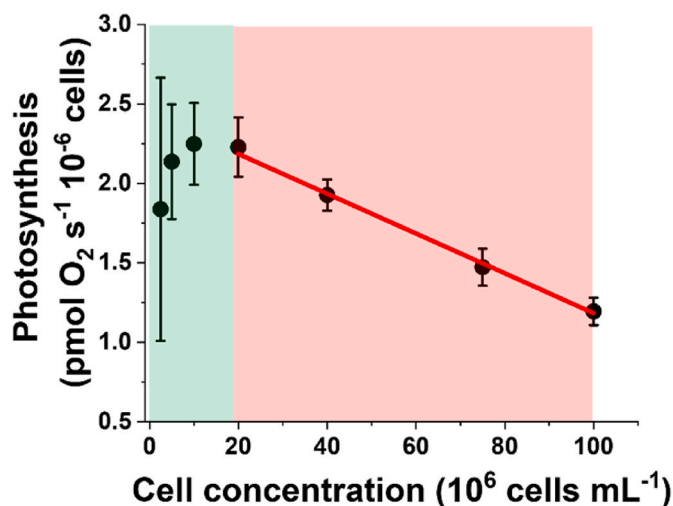


**Fig. 2. Photosynthetic activity as a function of cell concentration.** Photosynthesis is expressed as net rate of  $O_2$  evolution and it is normalized to the number of cells. The net rate of  $O_2$  evolution here reported corresponds to the values measured at  $50 \mu\text{mol photons m}^{-2} \text{s}^{-1}$  (i.e. an irradiance value neither limiting nor saturating for photosynthesis as reported in the PI curves of Supplementary Fig. S2) for *Nannochloropsis* samples with increasing cell concentration:  $2.5, 5, 10, 20, 40, 75$  and  $100 \cdot 10^6 \text{ cells mL}^{-1}$ , and corresponds to the star value in Fig. 1. The rate of  $O_2$  evolution is constant in the range  $2.5 \cdot 10^6 \text{ cells mL}^{-1} - 20 \cdot 10^6 \text{ cells mL}^{-1}$  (green area), whilst it decreases as the cell concentration increases between  $20 \cdot 10^6 \text{ cells mL}^{-1} - 100 \cdot 10^6 \text{ cells mL}^{-1}$  (red area). The slope of the linear correlation equation in the green area is not significantly different from 0 [ $y = (2.12 \pm 0.11) + (0.006 \pm 0.007) x$ , Pearson's R: 0.5,  $R^2$ : 0.25], whilst in the red area it is [ $y = (2.43 \pm 0.03) - (0.01 \pm 0.0004) x$ , Pearson's R: 0.99,  $R^2$ : 0.99 ( $t$ -Test,  $p$ -value  $< 0.05$ ). Data refer to the average  $\pm$  SD of four independent biological replicates.

$\text{mL}^{-1}$ , photosynthetic activity instead decreased as the cell concentration increased. This is likely to depend on the inhomogeneous light distribution in the samples because of their high optical density. Maximal gross photosynthesis values were equal for all concentrations measured, as expected since all cells are saturated. This confirms that the differences of photosynthetic activity observed at lower intensities depend on a shading effect (Supplementary Table S1).

### 3.3. Measuring photosynthetic functionality in dense microalgae cultures

To better assess how self-shading affected photosynthetic activity of *Nannochloropsis* cells, the photosynthesis-irradiance relationship of diluted and dense samples ( $5 \cdot 10^6 \text{ cells mL}^{-1}$  and  $100 \cdot 10^6 \text{ cells mL}^{-1}$ , respectively) were compared (Fig. 3).

We observed that the concentration of cells had a substantial effect on the shape of the photosynthesis-irradiance relationship, especially during the linear phase (Fig. 3a). The dark respiration rate ( $R_D$ ) of the densest sample ( $100 \cdot 10^6 \text{ cells mL}^{-1}$ ) was  $< 30\%$  of the value measured for the diluted sample ( $5 \cdot 10^6 \text{ cells mL}^{-1}$ , Fig. 3b), whilst no significant differences were observed for the light compensation point ( $I_{\text{comp}}$ ) (Fig. 3c). The reduction of  $R_D$  progressively followed the increase in the cell concentration (Supplementary Table S1) and we hypothesized that this might depend on a progressively lower diffusion efficiency of  $O_2$  in samples at increasing cell density. The light saturation point ( $I_{\text{sat}}$ ) was instead higher in the densest sample (Fig. 3d). This can be explained because of the higher optical density and cells shading in the sample, that thus requires stronger illumination to reach saturation. This hypothesis was confirmed by the observation that the maximal gross  $O_2$  photosynthetic rate ( $P_{\text{gmax}}$ ) was the same for both cell concentrations (Fig. 3e). The value of maximal gross photosynthesis is therefore reliably estimated even in dense microalgae samples, because when light is in excess the effect of self-shading becomes negligible since all cells are exposed to saturating illumination.

Overall, the methodology employed in this work enables the reliable estimation of photosynthetic parameters both in low and high optical density microalgae samples. In the second case, this enables to

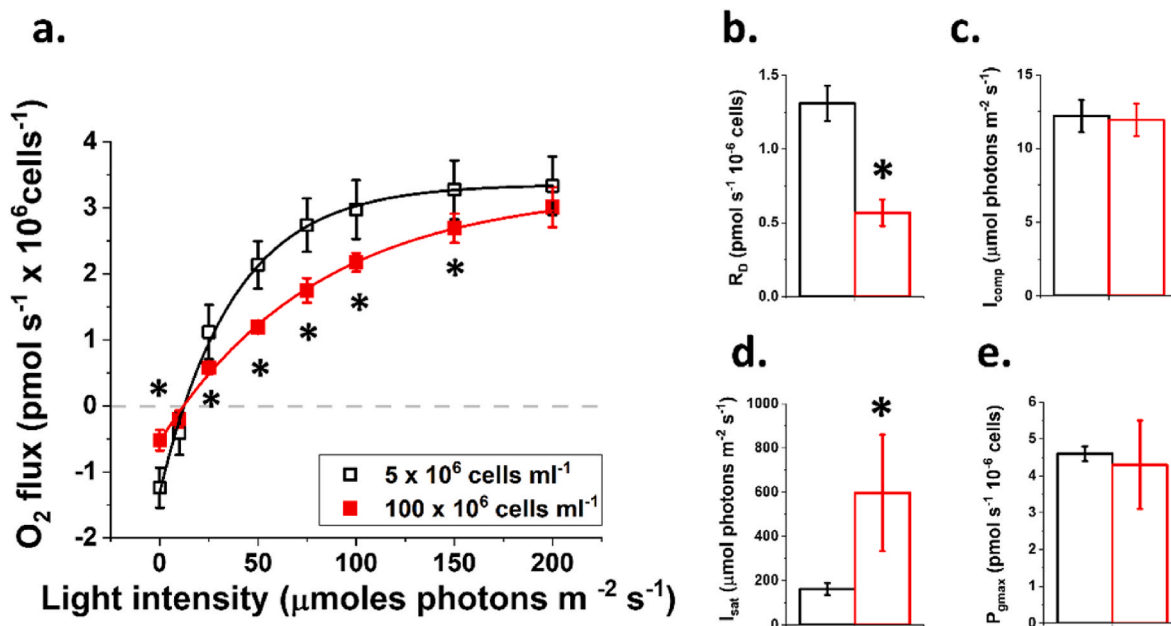


**Fig. 3. Photosynthesis-Irradiance dependance as a function of culture density.** The photosynthesis-Irradiance relationship was measured for diluted and dense *Nannochloropsis* cultures (i.e.  $5$  and  $100 \cdot 10^6 \text{ cells mL}^{-1}$ , respectively) and fitted with the equation defined in (Ye, 2007), using a minimum mean square error-based approach (a). The fitting returned the mathematical parameters indicated in panels from b) to e), that describe the differences in the shapes of the curves represented in panel a). For each mathematical parameter, the asterisk indicates a statistically significant difference between the two culture densities ( $t$ -Test,  $p$ -value  $< 0.05$ ). Data refer to the average  $\pm$  SD of four independent biological replicates. Black,  $5 \cdot 10^6 \text{ cells mL}^{-1}$  and red,  $100 \cdot 10^6 \text{ cells mL}^{-1}$  cell concentration. The same parameters for all the other cell concentrations tested in this work are reported in Supplementary Table S1.



extrapolate the photosynthetic performances of microalgae cultures, like those typical of industrially relevant cultivation plants, already at the lab-scale.

### 3.4. How does cell's light absorption capacity impact the Photosynthesis-Irradiance relationship in microalgae dense cultures?

The methodology described in this work offers the opportunity to investigate the photosynthetic activity of microalgae in complex light environments and quantitatively assess the impact of shading on photosynthetic activity. In the past few years, we successfully isolated *Nannochloropsis* mutants with different degrees of reduction in the Chl content [Fig. 4a (Perin et al., 2015)], which did not result in any affected phototrophic growth phenotype at the lab-scale (Fig. 4b). These strains indeed represent a useful tool to better describe how microalgae photosynthesis responds when shading effects, typical of cultivation in high optical-density conditions, become relevant.

In this work, we measured the photosynthesis-irradiance relationship of these microalgae strains and compared it to the reference parental *Nannochloropsis* strain, in both diluted and dense cultures (Fig. 5a and b). In this case, to account for the different Chl content of the strains under investigation, data were normalized on the Chl content (Fig. 5). It is in fact worth noting that in strains with a reduced light absorption capacity, the optimal chlorophyll concentration to achieve the maximal light absorption is reached at higher cell density than the parental strain (Formighieri et al., 2012), calling for a comparison on a Chl-basis. We observed that the effect of cell concentration on the shape of the photosynthesis-irradiance relationship, that we previously measured for the WT (Fig. 3a), is maintained also in photosynthetic pale mutants (Supplementary Table S3).

Also in this case, the dark respiration rate ( $R_D$ ) of dense cultures was lower than in diluted samples, with implications also on the light saturation point. Densest cultures showed a higher light saturation point than diluted samples, consistently with shading (Fig. 5a and b and Supplementary Table S3). Overall, these data suggest the photosynthetic mutant strains investigated in this work respond to the environmental conditions of dense cultures, as well as the parental strain.

In both diluted and dense cultures, the mutant strains here investigated showed an increase in the dark respiration rate ( $R_D$ ) with respect to the WT, as expected (Formighieri et al., 2012). No major differences in other photosynthetic parameters were instead observed between WT

and mutant strains in diluted conditions, whilst in dense cultures we observed a shared increase in  $P_{gmax}$ ,  $I_{comp}$  and  $I_{sat}$  (Supplementary Table S3), as expected on a Chl basis for Chl-less strains (Formighieri et al., 2012).

Strain I29, that, out of the four strains tested in this work, had the largest reduction in pigment content with respect to the WT, did not show any difference of photosynthetic functionality on a Chl-basis than the WT in diluted cultures (Fig. 5a). In dense cultures, I29 instead showed with equal cell concentration a higher photosynthetic activity than the WT at most of the tested irradiances, with the difference increasing with light intensity. In dense cultures, I29 also saturates photosynthesis at higher irradiances than the parental strain (Fig. 5b). These data suggest that mutants with a reduced pigment content show an improvement of photosynthetic functionality on a Chl-basis vs. the parental strain, but it depends on the density of the culture, where self-shading effects likely become relevant for photosynthesis.

To validate this hypothesis, we measured the Photosynthesis-Irradiance relationship of the other three pale mutants presented in Fig. 4. It is in fact worth noting that the four pale *Nannochloropsis* mutants of this work showed different degrees of reduction of pigment content (Fig. 4a), making them the ideal choice to assess the impact of a wide range of shading degrees because of differences in the cells' light absorption capacity. We observed that also the other three strains tested in this work showed an improved photosynthetic functionality on a Chl-basis with respect to the WT and that this phenomenon is observable only in dense cultures, but in these cases only at high irradiance (i.e. 400  $\mu\text{mol photons}\cdot\text{s}^{-1}\cdot\text{m}^{-2}$ , Supplementary Fig. S3). It is worth remembering that these strains showed a lower reduction of Chl content with respect to strain I29 (Fig. 4a). It is therefore likely that a reduced cell's light absorption capacity can drive an improved light distribution profile in a dense culture, but the latter phenomenon is understandably influenced by the presence of a relevant shading effect, which in turn depends not only on the culture density alone, but also on the incident light.

To validate the latter conclusion, we plotted the improvement of photosynthetic activity measured at 50  $\mu\text{mol photons}\cdot\text{s}^{-1}\cdot\text{m}^{-2}$  (i.e. expressed as percentage with respect to the photosynthetic activity of the WT), for the four pale mutants investigated this work, versus the reduction of pigment content, as percentage of the pigment content of the WT (Supplementary Fig. S4) and compared diluted and dense cultures. 50  $\mu\text{mol photons}\cdot\text{s}^{-1}\cdot\text{m}^{-2}$  was chosen for an unbiased comparison between strains because it does not fall either within the limiting or

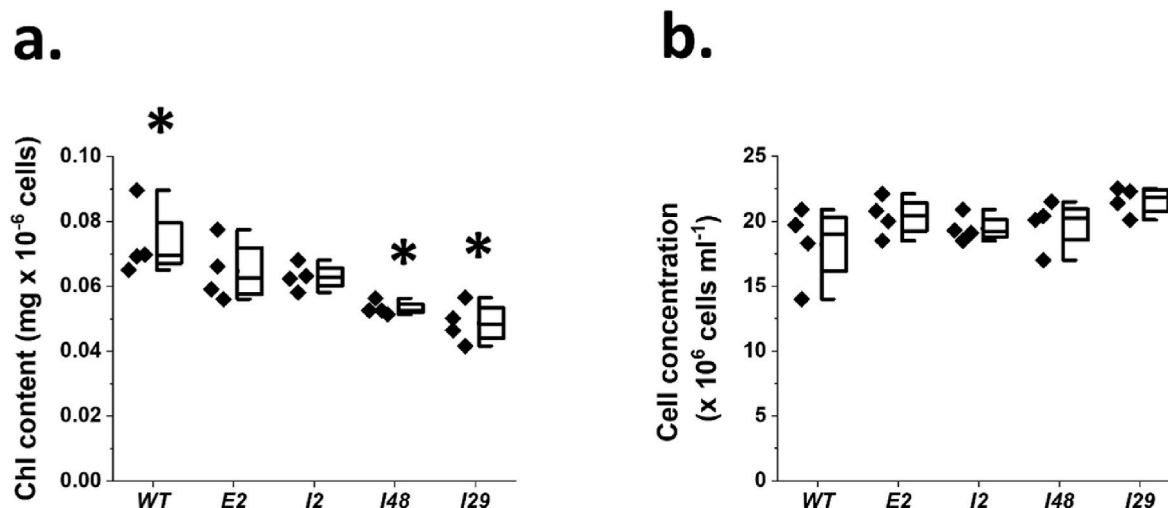
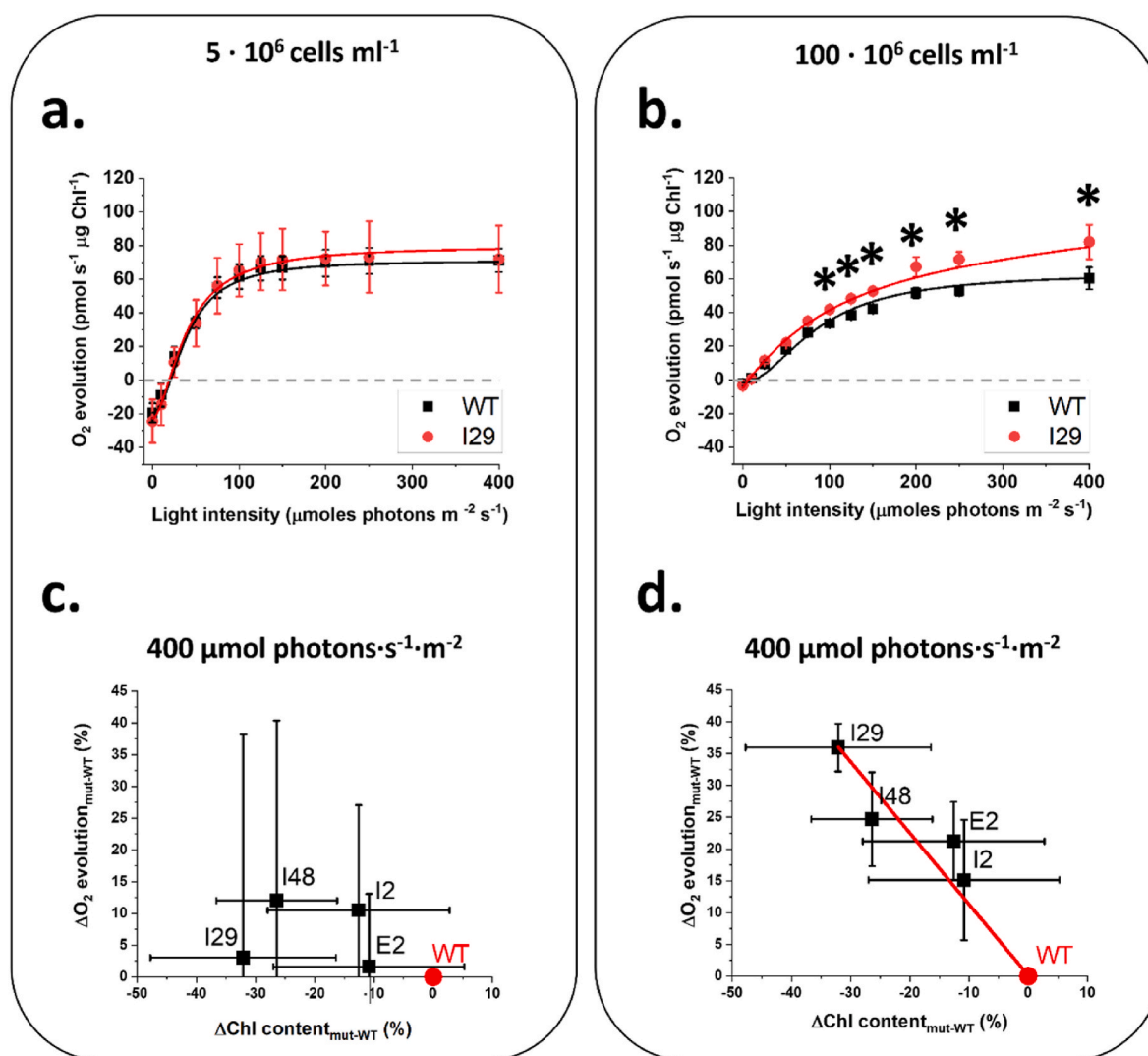


Fig. 4. *Nannochloropsis* mutants with a reduced chlorophyll content and unaffected phototrophic growth. *Nannochloropsis* mutants showing different degrees of reduction of chlorophyll (Chl) content (a), but unaffected phototrophic growth (b) with respect to the parental strain (WT) were isolated (Perin et al., 2015). Data refer to the average  $\pm$  SD of four independent biological replicates, grown in plastic cell culture flasks with ventilation caps for four days, according to the protocol detailed in the materials and methods section. Asterisks indicate statistically significant differences between one mutant and the parental strain (*t*-Test, *p*-value < 0.05).



**Fig. 5. Improvement of photosynthetic activity on a Chl-basis as a function of the reduction of the pigment content, in *Nannochloropsis* cultures with different densities.** Examples of Photosynthesis-Irradiance relationship measured for *Nannochloropsis* WT and I29 strain, showing 30% reduction of Chl content with respect to the former (Fig. 4a), in diluted (a) (i.e.  $5 \cdot 10^6 \text{ cells ml}^{-1}$ ) and dense (b) (i.e.  $100 \cdot 10^6 \text{ cells ml}^{-1}$ ) cultures on a Chl-basis to account for the differences in the chlorophyll content per cell, as reported in Fig. 4a. Data were fitted with the equation of (Ye, 2007) using a minimum mean square error-based approach. Improvement in the rate of  $\text{O}_2$  evolution at  $400 \mu\text{mol photons s}^{-1} \text{m}^{-2}$ , expressed as percentage with respect to the value of the parental strain (WT) for the four mutants showing different degrees of reduction in the chlorophyll (Chl) content, expressed as percentage of reduction with respect to the WT, for diluted (i.e.  $5 \cdot 10^6 \text{ cells ml}^{-1}$ ) (c) and dense (i.e.  $100 \cdot 10^6 \text{ cells ml}^{-1}$ ) (d) *Nannochloropsis* cultures. Data correspond to the photosynthetic activity measured at  $400 \mu\text{mol photons}\cdot\text{s}^{-1}\cdot\text{m}^{-2}$ , that is the irradiance to which dense cultures in lab-scale PBRs demonstrated an improved biomass productivity (Perin et al., 2017a). There isn't linear correlation between x and y observations in panel c), whilst there is linear correlation in panel d) (red continuous line), (*t*-Test, *p*-value < 0.05). Parametric values for the correlation equations for the two panels are reported in Supplementary Table S2. Data refer to the average  $\pm$  SD of four independent biological replicates. Asterisks indicate statistically significant differences between one mutant and the parental strain (*t*-Test, *p*-value < 0.05). The original data used in this figure are reported in Supplementary Fig. S3.

saturating ranges for photosynthesis (Fig. 1).

We observed that at this irradiance there wasn't any improvement of photosynthetic activity for any of the four strains here investigated in diluted conditions with respect to the WT (Supplementary Fig. S4a). Strain I29 was the only one to show an improved photosynthetic activity on a Chl-basis in dense conditions, but overall, there was no relevant linear correlation between improvement in photosynthetic activity and reduction of pigment content either (Supplementary Fig. S4b).

When we plotted the improvement of photosynthetic activity measured at  $400 \mu\text{mol photons}\cdot\text{s}^{-1}\cdot\text{m}^{-2}$ , versus the reduction of pigment content for the four pale mutants investigated this work, instead we observed a significant difference between diluted and dense conditions. In diluted cultures there was no improvement in photosynthetic activity (Fig. 5c), whilst in dense conditions, there was a significant correlation

between improvement in photosynthetic functionality on a Chl-basis and reduction in pigment content, with the greatest reduction of the latter leading to the greatest improvement of photosynthetic activity (Fig. 5d).

It is worth mentioning that the strains investigated in this work showed an improved biomass productivity in dense lab-scale PBR cultures exposed at  $400 \mu\text{mol photons}\cdot\text{s}^{-1}\cdot\text{m}^{-2}$  indeed, with the intensity of the measured advantage directly proportional to the level of reduction in the Chl content (e.g. strain I29 showed the strongest effect) (Perin et al., 2017a).

Overall, these data demonstrate that photosynthetic activity is affected by the cultivation conditions, with shading effects of dense cultures making a substantial difference with respect to diluted conditions. Shading effects can be effectively reduced by decreasing cell's

light absorption capacity, leading to a significant improvement in light distribution and consequently photosynthetic activity, provided enough photons are used to drive an inhomogeneous light distribution profile in dense WT microalgae cultures.

## 4. Discussion

### 4.1. Estimation of PI relationship in both diluted and dense microalgae cultures

Molecular oxygen is a by-product of photosynthesis, and its concentration is directly proportional to the number of electrons that are vehiculated through the photosynthetic electron transport chain, making the rate of O<sub>2</sub> evolution a good choice for the investigation of photosynthetic functionality.

The quantification of the concentration of molecular oxygen is often reached with devices based on Clark-type electrodes, yet the information achievable is being often limited by the i) low resolution and sensitivity and ii) difficulty in the precise control of light supply to the sample. Among real-time non-invasive methods, optical sensors are representing an important alternative to overcome the former limitations, with optodes standing out for the possibility to measure with high precision also more than one analyte at a time (e.g. O<sub>2</sub> and CO<sub>2</sub>). However, optodes require molecular sensors to interact with oxygen and undergo an O<sub>2</sub>-dependent change in their optical properties, often showing a limited linearity range that affects versatility (Staudinger et al., 2018; Kalinichev et al., 2024).

To improve resolution and sensitivity to light-induced O<sub>2</sub>-changes, in this work we used one high-sensitivity Clark electrode and demonstrated that it can detect the concentration of molecular oxygen in very-low-concentration samples (e.g.  $1 \cdot 10^6$  cells ml<sup>-1</sup> and  $2.5 \cdot 10^6$  cells ml<sup>-1</sup>, Supplementary Fig. S2) in *Nannochloropsis*. These concentration values are on average 30 times lower than those used with alternative Clark sensors (Ben-Sheleg et al., 2021; Perin et al., 2015; Vonshak et al., 2020), minimizing the volume of microalgae culture to sacrifice for the evaluation of photosynthetic activity. More importantly, the investigation of photosynthetic functionality at low cell concentration opens the possibility to investigate cultures with minimal shading.

Indeed, we were able to assess the impact of different cell densities on microalgae photosynthetic functionality. When we compared the Photosynthesis-Irradiance (PI) relationship of *Nannochloropsis* cultures at different concentrations, from diluted (i.e.  $5 \cdot 10^6$  cells ml<sup>-1</sup>) to dense ( $100 \cdot 10^6$  cells ml<sup>-1</sup>), we observed that there was an effect of cell density on the shape of the PI curve (Fig. 3a). At non-saturating irradiances [ $<150 \mu\text{mol photons}\cdot\text{s}^{-1}\cdot\text{m}^{-2}$  for *Nannochloropsis* (Sforza et al., 2012)], the photosynthetic activity was lower in dense cultures, indeed suggesting the high cell concentration triggers an inhomogeneous light distribution profile within the sample, with a substantial fraction of cells exposed to limiting light and thus not receiving enough energy to drive photochemistry. Nevertheless, maximal gross photosynthesis in the high-density sample equals the diluted culture, indicating the method could still reliably estimate photosynthetic parameters even in dense microalgae cultures (Fig. 3e), enabling extrapolation of photosynthetic performances in cultivation conditions typical of industrial systems already at the lab-scale.

### 4.2. Cells' light absorption capacity affects photosynthetic functionality in dense microalgae cultures

The method employed in this work enables to quantitatively assess the impact of cell's self-shading on microalgae photosynthetic activity. To investigate this phenomenon in detail, we used as validation tools *Nannochloropsis* strains with an altered Chl content with respect to the parental strain and measured their PI relationship at increasing cell densities.

The PI determinations of this work were performed using blue light,

that is efficiently absorbed by chlorophyll, generating a slightly steeper light attenuation profile than with white light. However, it should be noted that photosynthetic activity depends on the photon fluxes rather than their energy and that all visible light is eventually absorbed by Chl (Liu and van Iersel, 2021), making the results discussed in the work relevant also for microalgae cultivated upon natural sunlight.

We used four *Nannochloropsis* strains, previously isolated for a reduced Chl content and unaffected phototrophic growth (Fig. 4) and measured their PI curves using one high-sensitivity Clark electrode, comparing diluted and dense cultures (Fig. 5). We observed that all mutant strains responded to the culture density as well as the WT and showed a reduction of the dark respiration rate (R<sub>D</sub>) and an increase of I<sub>sat</sub> as the density increased (Supplementary Table S3). We observed that the reduction of R<sub>D</sub> progressively followed the increase in the cell density (Supplementary Table S1), suggesting this may depend on a progressively lower diffusion efficiency of O<sub>2</sub> in the sample as the cell density increased, even if the mixing rate was optimal according to the manufacturer (see Materials and Methods).

In both diluted and dense conditions, the mutant strains showed an increased dark respiration rate (R<sub>D</sub>), I<sub>comp</sub>, I<sub>sat</sub> and P<sub>gmax</sub> with respect to the WT, as expected on a Chl basis from prediction models for Chl-less mutants (Formighieri et al., 2012).

At low light (i.e.  $50 \mu\text{mol photons}\cdot\text{s}^{-1}\cdot\text{m}^{-2}$ ), we didn't observe any improvement of photosynthetic activity either in diluted or dense cultures (Supplementary Fig. S4), suggesting that the cell concentration and the number of photons, respectively in diluted and dense conditions, were not high enough to drive a significant difference in the light distribution profile between mutants and WT cultures. To validate this hypothesis, we estimated a simplified light distribution profile within lab-scale PBRs (Supplementary Fig. S5 and Fig. 6) starting from transmittance data experimentally determined (Supplementary Table S4) and assuming the light absorption followed the Lambert-Beer law (Fernández et al., 1997). Upon  $50 \mu\text{mol photons}\cdot\text{s}^{-1}\cdot\text{m}^{-2}$ , in diluted conditions, the WT culture is overall receiving more photons than in dense conditions. In the latter, half of the culture volume is below the light compensation point (grey area) and is indeed predicted to have negative productivity (Supplementary Figs. S5b and S5c). At low light, both in diluted (i.e.  $5 \cdot 10^6$  cells ml<sup>-1</sup>) and dense (i.e.  $100 \cdot 10^6$  cells ml<sup>-1</sup>) conditions, the mutant strain I29, showing the strongest reduction in pigment content vs the WT, is predicted to have the same light attenuation profile than the parental strain within a tubular PBR with a 5 cm diameter (Supplementary Figs. S5b and S5c), confirming the results of the PI curves measured in this work in which we didn't observe any improvement in such experimental conditions (Fig. 5a).

At saturating light (i.e.  $400 \mu\text{mol photons}\cdot\text{s}^{-1}\cdot\text{m}^{-2}$ ), we still did not observe any significant difference in photosynthetic activity vs the WT for any of the four strains here investigated in diluted samples (Fig. 5c), whilst in dense cultures we observed a significant improvement in the rate of O<sub>2</sub> evolution on a Chl-basis with respect to the parental strain. Such improvement progressively increased with the reduction of the Chl content (Fig. 5d).  $400 \mu\text{mol photons}\cdot\text{s}^{-1}\cdot\text{m}^{-2}$  is the irradiance at which the four mutant strains indeed showed an improved biomass productivity than the WT in the high density condition tested in this work, following the degree of reduction in the Chl content (Perin et al., 2017a). This is likely to depend on a more homogeneous light distribution in dense cultures of microalgae with a reduced Chl content because of a reduced self-shading, with more light reaching the cells most distal from the light source than in WT cultures (Formighieri et al., 2012; Perin et al., 2019).

This phenomenon is expected to drive a higher photochemical rate in regions of the culture volume with less light availability, with beneficial consequences on the growth of the whole mass culture. Such improvement is observable only in dense cultures, because in diluted conditions light is available to all cells also in the case of the WT.

The simplified model of the light attenuation profile indeed suggests that, upon light saturation, whilst in diluted conditions both the WT and

the mutant strain are experiencing the same light attenuation profile (Supplementary Fig. S5a), in dense conditions the WT attenuates light faster and the last 0.5 cm of the culture volume from the light source is predicted to receive light below the compensation point and to have consequently negative productivity (Fig. 6). In dense conditions, the reduction in the pigment content of the I29 strain drives to a slower light attenuation profile and the culture is overall predicted to be exposed to more photons than the WT, preventing regions at negative productivity (Fig. 6), providing a possible explanation behind the observed improvement in the photosynthetic rate at saturating irradiances in dense cultures vs the WT from PI curves.

The same calculations also enabled to hypothesize why the improvement of the photosynthetic rate in such operational conditions was proportional to the reduction of the chlorophyll content, as observed in Fig. 5d. The other three mutants exploited in this work are predicted to have an improved light penetration profile within the mass culture vs the WT indeed (Supplementary Fig. S6), yet their reduction in the pigment content is not enough to prevent regions at negative productivity, which however are progressively smaller than in the WT, following the reduction in the pigment content.

In mutants E2, I48 and I29 the loss of pigment comes from a significant reduction of the antenna proteins of Photosystems II (PSII) while in mutant I2 the pigment loss instead depends on a reduction of all pigment binding complexes, including reaction centers (Bellan et al., 2020; Perin et al., 2015, 2023). The phenomena here described are thus more strongly connected with the culture's light absorption capacity and the specific pigment binding complexes affected appears to have a smaller effect.

Along the rationale that a reduced pigment content can improve the light distribution profile within a mass culture, in the past years, several research efforts were successfully devoted to the isolation of paler microalgae strains, in different species. In controlled lab-scale conditions, these strains were demonstrated to increase light-use efficiency and growth with respect to the reference parental strains indeed (Cazzaniga et al., 2014; Dall'Osto et al., 2019; Kirst et al., 2012; Kirst and Melis, 2014; Mussnug et al., 2005; Perin et al., 2015). Also the four mutant strains used in this work were demonstrated to have an improved biomass productivity in lab-scale PBRs (Perin et al., 2017a).

However, once pale mutant strains were tested at a higher cultivation scale (e.g. pilot plants outdoors), mixed results were obtained, with

the confirmation of a growth advantage in some cases (Cazzaniga et al., 2014), but not in others (De Mooij et al., 2014). This phenomenon is yet to be fully addressed but is shedding light on the role played by the cultivation environment on photosynthesis. As observed e.g. for domesticated *Nannochloropsis* strains (Perin et al., 2017b), photosynthetic phenotypes acclimate to the cultivation environment and they can respond with a different intensity than the corresponding parental strain. Consequently, the cultivation environment, in some cases, can even mask the photosynthetic features isolated at the lab-scale and the original advantage can be lost. This discrepancy of behaviors from the lab-to the industrial-scale of cultivation has been under-investigated so far, mainly because most of the phenomena impacting microalgae photosynthesis in photobioreactors can only be assessed at scale (Masojtdek et al., 2021), calling for, often unbearable, economic efforts.

The methodology exploited in this work opens the possibility to extrapolate the photosynthetic functionality of microalgae in dense cultures typical of industrial cultivation plants already at the lab-scale, enabling the collection of relevant information without any additional cost and ultimately allowing the development of more robust biotechnological optimization efforts.

## 5. Conclusions

Photosynthesis is affected by the available irradiance and understanding how the former responds to the latter has both important natural and biotechnological implications.

Culture's density has a substantial effect on microalgae photosynthetic activity. The highest the cell's light absorption capacity, the greatest the effect on photosynthesis on a Chl-basis. Reducing the cell's pigment content has been demonstrated to bring an advantage in dense microalgae cultures indeed, likely because of a more homogeneous light distribution profile, provided the environmental conditions drive to a relevant shading effect in WT cultures. High-sensitivity oxygen measurements are informative to understand how photosynthesis responds to culture density, opening the possibility to extrapolate already at the lab scale performances of industrial microalgae cultures and speeding up the identification of robust biological targets for biotechnological optimization.

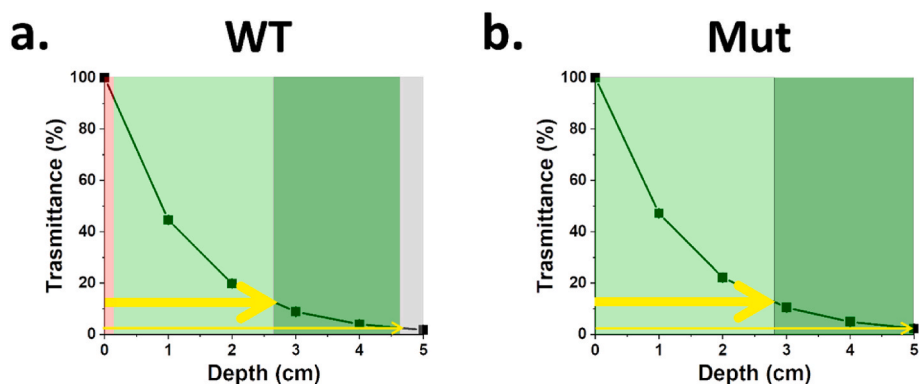


**Fig. 6. Light distribution profile in microalgae cultures.** Estimation of the light attenuation profile for *Nannochloropsis* cultures of both WT and the strain I29 (i.e. Mut), showing the strongest reduction in Chl content vs the former, upon cultivation in tubular PBR of 5 cm diameter, in dense (i.e.  $100 \cdot 10^6$  cells  $\text{ml}^{-1}$ ) conditions, and illuminated from one side with saturating (i.e.  $400 \mu\text{mol photons} \cdot \text{s}^{-1} \cdot \text{m}^{-2}$ ) light. The light intensity attenuation profile (expressed as transmittance, namely the ratio between transmitted/incident light intensities), was estimated using the Lambert-Beer law (Fernández et al., 1997) and it was calculated from the values of transmitted light intensity experimentally measured after 5 cm of culture (Supplementary Table S4). Graphs are divided in areas of different colors, according to the light intensity reaching cells populating different culture layers, using the PI curves data experimentally measured in this work and consistently to the definitions of Fig. 1. Red, regions above the light saturation point with high biomass productivity and low photosynthetic efficiency (PE); Light green, regions between light saturation and  $50 \mu\text{mol photons s}^{-1} \text{m}^{-2}$  at high biomass productivity and high PE (highlighted by the thicker yellow arrow); Dark green, regions between  $50 \mu\text{mol photons s}^{-1} \text{m}^{-2}$  and the light compensation point at low biomass productivity and high PE (highlighted by the thinner yellow arrow); Grey, regions below the light compensation point at biomass consumption and negative productivity. The calculations of the light attenuation profile in the other operational conditions are reported in Supplementary Fig. S5, whilst the other mutant strains exploited in this work are reported in Supplementary Fig. S6.



## Funding

GP acknowledges the support from the University of Padova STARS Project WWBiomass. TM acknowledges the support from European Union H2020 Projects No. 859770-NextGen-O2k and Marie Skłodowska-Curie No. 955520 Digitalgae.

## CRediT authorship contribution statement

**Antoni Mateu Vera-Vives:** Data curation, Formal analysis, Methodology, Writing – original draft. **Tim Michelberger:** Data curation, Methodology. **Tomas Morosinotto:** Conceptualization, Funding acquisition, Writing – review & editing. **Giorgio Perin:** Conceptualization, Data curation, Formal analysis, Funding acquisition, Supervision, Validation, Writing – original draft, Writing – review & editing.

## Declaration of competing interest

The authors declare that they have no known competing financial interests or personal relationships that could have appeared to influence the work reported in this paper.

## Data availability

Data will be made available on request.

## Appendix A. Supplementary data

Supplementary data to this article can be found online at <https://doi.org/10.1016/j.plaphy.2024.108510>.

## References

- Bellan, A., Bucci, F., Perin, G., Alboresi, A., Morosinotto, T., 2020. Photosynthesis regulation in response to fluctuating light in the secondary endosymbiont alga *Nannochloropsis gaditana*. *Plant Cell Physiol.* 61 <https://doi.org/10.1093/pcp/pcz174>.
- Ben-Sheleg, A., Khozin-Godberg, I., Yaakov, B., Vonshak, A., 2021. Characterization of *Nannochloropsis oceanica* rose bengal mutants sheds light on acclimation mechanisms to high light when grown in low temperature. *Plant Cell Physiol.* 62, 1478–1493. <https://doi.org/10.1093/pcp/pcab094>.
- Cavicchioli, R., Ripple, W.J., Timmis, K.N., Azam, F., Bakken, L.R., Baylis, M., Behrenfeld, M.J., Boetius, A., Boyd, P.W., Classen, A.T., Crowther, T.W., Danovaro, R., Foreman, C.M., Huisman, J., Hutchins, D.A., Jansson, J.K., Karl, D.M., Koscella, B., Mark Welch, D.B., Martiny, J.B.H., Moran, M.A., Orphan, V.J., Reay, D.S., Remais, J.V., Rich, V.I., Singh, B.K., Stein, L.Y., Stewart, F.J., Sullivan, M.B., van Oppen, M.J.H., Weaver, S.C., Webb, E.A., Webster, N.S., 2019. Scientists' warning to humanity: microorganisms and climate change. *Nat. Rev. Microbiol.* 17, 569–586. <https://doi.org/10.1038/s41579-019-0222-5>.
- Cazzaniga, S., Dall'Osto, L., Szaub, J., Scibilia, L., Ballottari, M., Purton, S., Bassi, R., 2014. Domestication of the green alga *Chlorella sorokiniana*: reduction of antenna size improves light-use efficiency in a photobioreactor. *Biotechnol. Biofuels* 7, 157. <https://doi.org/10.1186/s13068-014-0157-z>.
- Dall'Osto, L., Cazzaniga, S., Guardini, Z., Barera, S., Benedetti, M., Mannino, G., Maffei, M.E., Bassi, R., 2019. Combined resistance to oxidative stress and reduced antenna size enhance light-to-biomass conversion efficiency in *Chlorella vulgaris* cultures. *Biotechnol. Biofuels* 12, 221. <https://doi.org/10.1186/s13068-019-1566-9>.
- De Mooij, T., Janssen, M., Cerezo-Chinarro, O., Mussgnug, J.H., Kruse, O., Ballottari, M., Bassi, R., Bujaldon, S., Wollman, F.-A., Wijffels, R.H., 2014. Antenna size reduction as a strategy to increase biomass productivity: a great potential not yet realized. *J. Appl. Phycol.* <https://doi.org/10.1007/s10811-014-0427-y>.
- de Souza Kirnev, P.C., de Souza Vandenberghe, L.P., Socolo, C.R., de Carvalho, J.C., 2022. Chapter 2 - mixing and agitation in photobioreactors. In: Thatoi, H., Mohapatra, S., Das, S.K. (Eds.), *Innovations in Fermentation and Phytopharmaceutical Technologies*. Elsevier, pp. 13–35. <https://doi.org/10.1016/B978-0-12-821877-8.00005-1>.
- Doerrier, C., Garcia-Souza, L.F., Krumschnabel, G., Wohlfarter, Y., Mészáros, A.T., Gnaiger, E., 2018. High-resolution Fluorescence Respirometry and OXPHOS protocols for human cells, permeabilized fibers from small biopsies of muscle, and isolated mitochondria. *Methods Mol. Biol.* 1782, 31–70. [https://doi.org/10.1007/978-1-4939-7831-1\\_3](https://doi.org/10.1007/978-1-4939-7831-1_3).
- Fernández, F.G.A., Camacho, F.G., Pérez, J.A.S., Sevilla, J.M.F., Grima, E.M., 1997. A model for light distribution and average solar irradiance inside outdoor tubular photobioreactors for the microalgal mass culture. *Biotechnol. Bioeng.* 55, 701–714. [https://doi.org/10.1002/\(SICI\)1097-0290\(19970905\)55:5<701::AID-BIT1>3.0.CO;2-F](https://doi.org/10.1002/(SICI)1097-0290(19970905)55:5<701::AID-BIT1>3.0.CO;2-F).
- Formighieri, C., Franck, F., Bassi, R., 2012. Regulation of the pigment optical density of an algal cell: filling the gap between photosynthetic productivity in the laboratory and in mass culture. *J. Biotechnol.* 162, 115–123. <https://doi.org/10.1016/j.biotech.2012.02.021>.
- Gnaiger, E., 2001. Bioenergetics at low oxygen: dependence of respiration and phosphorylation on oxygen and adenosine diphosphate supply. *Respir. Physiol.* 128, 277–297. [https://doi.org/10.1016/S0034-5687\(01\)00307-3](https://doi.org/10.1016/S0034-5687(01)00307-3).
- Gnaiger, E., 2008. Polarographic oxygen sensors, the oxygraph, and high-resolution respirometry to assess mitochondrial function. In: *Drug-Induced Mitochondrial Dysfunction*. John Wiley & Sons, Ltd, pp. 325–352. <https://doi.org/10.1002/9780470372531.ch12>.
- Guillard, R.R.L., Ryther, J.H., 1962. Studies of marine planktonic diatoms: I. *Cyclotella* NANA HUSTEDT, and *detonula confervacea* (cleve) gran. *Can. J. Microbiol.* 8, 229–239. <https://doi.org/10.1139/m62-029>.
- Guiry, M.D., 2012. How many species of algae are there? *J. Phycol.* 48, 1057–1063. <https://doi.org/10.1111/j.1529-8817.2012.01222.x>.
- Heaton, E.A., Dohleman, F.G., Long, S.P., 2008. Meeting US biofuel goals with less land: the potential of *Miscanthus*. *Global Change Biol.* 14, 2000–2014. <https://doi.org/10.1111/j.1365-2486.2008.01662.x>.
- Kalinichev, V., Zieger, S., A.E., Koren, K., 2024. Optical sensors (optodes) for multiparameter chemical imaging: classification, challenges, and prospects. *Analyst* 149, 29–45. <https://doi.org/10.1039/D3AN01661G>.
- Khan, M.I., Shin, J.H., Kim, J.D., 2018. The promising future of microalgae: current status, challenges, and optimization of a sustainable and renewable industry for biofuels, feed, and other products. *Microb. Cell Factories* 17, 36. <https://doi.org/10.1186/s12934-018-0879-x>.
- Kirchman, D.L., 2018. Microbial primary production and phototrophy, 0. In: Kirchman, D.L. (Ed.), *Processes in Microbial Ecology*. Oxford University Press. <https://doi.org/10.1093/oso/9780198789406.003.0006>.
- Kirst, H., Melis, A., 2014. The chloroplast signal recognition particle (CpSRP) pathway as a tool to minimize chlorophyll antenna size and maximize photosynthetic productivity. *Biotechnol. Adv.* 32, 66–72. <https://doi.org/10.1016/j.biotechadv.2013.08.018>.
- Kirst, H., Garcia-Cerdan, J.G., Zurbriggen, A., Ruehle, T., Melis, A., 2012. Truncated photosystem chlorophyll antenna size in the green microalga *Chlamydomonas reinhardtii* upon deletion of the TLA3-CpSRP43 gene. *Plant Physiol.* 160, 2251–2260. <https://doi.org/10.1104/pp.112.206672>.
- Liu, J., van Iersel, M.W., 2021. Photosynthetic physiology of blue, green, and red light: light intensity effects and underlying mechanisms. *Front. Plant Sci.* 12.
- Ma, Z., Cheah, W.Y., Ng, I.-S., Chang, J.-S., Zhao, M., Show, P.L., 2022. Microalgae-based biotechnological sequestration of carbon dioxide for net zero emissions. *Trends Biotechnol.* 40, 1439–1453. <https://doi.org/10.1016/j.tibtech.2022.09.002>.
- Masojídek, J., Ránglová, K., Lakatos, G.E., Silva Benavides, A.M., Torzillo, G., 2021. Variables governing photosynthesis and growth in microalgae mass cultures. *Processes* 9, 820. <https://doi.org/10.3390/pr9050820>.
- MiPNet MiPNet22.11 O2k-FluoRespirometer manual - Bioblast [WWW Document], n.d. URL [https://wiki.orooboros.at/index.php/MiPNet22.11\\_O2k-FluoRespirometer\\_manual](https://wiki.orooboros.at/index.php/MiPNet22.11_O2k-FluoRespirometer_manual) (accessed January.23.2024).
- Molazadeh, M., Ahmadzadeh, H., Pourianfar, H.R., Lyon, S., Rampelotto, P.H., 2019. The use of microalgae for coupling wastewater treatment with CO<sub>2</sub> biofixation. *Front. Bioeng. Biotechnol.* 7.
- Morgan-Kiss, R.M., Priscu, J.C., Pockock, T., Gudynaite-Savitch, L., Huner, N.P.A., 2006. Adaptation and acclimation of photosynthetic microorganisms to permanently cold environments. *Microbiol. Mol. Biol. Rev.* : MMBR (Microbiol. Mol. Biol. Rev.) 70, 222–252. <https://doi.org/10.1128/MMBR.70.1.222-252.2006>.
- Mussgnug, J.H., Wobbe, L., Elles, I., Claus, C., Hamilton, M., Fink, A., Kahmann, U., Kapazoglou, A., Mullineaux, C.W., Hippler, M., Nickelsen, J., Nixon, P.J., Kruse, O., 2005. NAB1 is an RNA binding protein involved in the light-regulated differential expression of the light-harvesting antenna of *Chlamydomonas reinhardtii*. *Plant Cell* 17, 3409–3421. <https://doi.org/10.1105/tpc.105.035774>.
- Olabi, A.G., Shehata, N., Sayed, E.T., Rodriguez, C., Anyanwu, R.C., Russell, C., Abdelkareem, M.A., 2023. Role of microalgae in achieving sustainable development goals and circular economy. *Sci. Total Environ.* 854, 158689 <https://doi.org/10.1016/j.scitotenv.2022.158689>.
- Perin, G., Morosinotto, T., 2019a. Potential of Microalgae Biomass for the Sustainable Production of Bio-Commodities. Springer, Cham, pp. 243–276. [https://doi.org/10.1007/124\\_2019\\_30](https://doi.org/10.1007/124_2019_30).
- Perin, G., Morosinotto, T., 2019b. Optimization of microalgae photosynthetic metabolism to close the gap with potential productivity. In: *Grand Challenges in Biology and Biotechnology*. Springer Science and Business Media B.V., pp. 223–248. [https://doi.org/10.1007/978-3-030-25233-5\\_6](https://doi.org/10.1007/978-3-030-25233-5_6).
- Perin, G., Morosinotto, T., 2023. Understanding Regulation in Complex Environments: A Route to Enhance Photosynthetic Light-Reactions in Microalgae Photobioreactors 1. <https://doi.org/10.3389/fphbi.2023.1274525>.
- Perin, G., Bellan, A., Segalla, A., Meneghesso, A., Alboresi, A., Morosinotto, T., 2015. Generation of random mutants to improve light-use efficiency of *Nannochloropsis gaditana* cultures for biofuel production. *Biotechnol. Biofuels* 8, 161. <https://doi.org/10.1186/s13068-015-0337-5>.
- Perin, G., Bernardi, A., Bellan, A., Bezzo, F., Morosinotto, T., 2017a. A mathematical model to guide genetic engineering of photosynthetic metabolism. *Metab. Eng.* 44, 337–347. <https://doi.org/10.1016/j.ymben.2017.11.002>.
- Perin, G., Simionato, D., Bellan, A., Carone, M., Occhipinti, A., Maffei, M.E., Morosinotto, T., 2017b. Cultivation in industrially relevant conditions has a strong influence on biological properties and performances of *Nannochloropsis gaditana* genetically modified strains. *Algal Res.* 28, 88–99. <https://doi.org/10.1016/j.algal.2017.10.013>.

- Perin, G., Bellan, A., Bernardi, A., Bezzo, F., Morosinotto, T., 2019. The potential of quantitative models to improve microalgae photosynthetic efficiency. *Physiol. Plantarum* 166. <https://doi.org/10.1111/ppl.12915>.
- Perin, Giorgio, Yunus, I.S., Valton, M., Alobwede, E., Jones, P.R., 2019. Sunlight-driven recycling to increase nutrient use-efficiency in agriculture. *Algal Res.* 41, 101554 <https://doi.org/10.1016/j.algal.2019.101554>.
- Perin, G., Gambaro, F., Morosinotto, T., 2022. Knowledge of regulation of photosynthesis in outdoor microalgae cultures is essential for the optimization of biomass productivity. *Front. Plant Sci.* 13 <https://doi.org/10.3389/FPLS.2022.846496>.
- Perin, G., Bellan, A., Michelberger, T., Lyska, D., Wakao, S., Niyogi, K.K., Morosinotto, T., 2023. Modulation of xanthophyll cycle impacts biomass productivity in the marine microalga *Nannochloropsis*. *Proc. Natl. Acad. Sci. U. S. A.* 120, e2214119120 <https://doi.org/10.1073/pnas.2214119120>.
- Ruiz, J., Olivieri, G., de Vree, J., Bosma, R., Willems, P., Reith, J.H., Eppink, M.H.M., Kleinegris, D.M.M., Wijffels, R.H., Barbosa, M.J., 2016. Towards industrial products from microalgae. *Energy Environ. Sci.* 9, 3036–3043. <https://doi.org/10.1039/C6EE01493C>.
- Schediwi, K., Trautmann, A., Steinweg, C., Posten, C., 2019. Microalgal kinetics — a guideline for photobioreactor design and process development. *Eng. Life Sci.* 19, 830–843. <https://doi.org/10.1002/elsc.201900107>.
- Sforza, E., Simionato, D., Giacometti, G.M., Bertucco, A., Morosinotto, T., 2012. Adjusted light and dark cycles can optimize photosynthetic efficiency in algae growing in photobioreactors. *PLoS One* 7, e38975. <https://doi.org/10.1371/journal.pone.0038975>.
- Staudinger, C., Strobl, M., Fischer, J.P., Thar, R., Mayr, T., Aigner, D., Müller, B.J., Müller, B., Lehner, P., Mistlberger, G., Fritzsche, E., Ehgartner, J., Zach, P.W., Clarke, J.S., Geißler, F., Mutzberg, A., Müller, J.D., Achterberg, E.P., Borisov, S.M., Klimant, I., 2018. A versatile optode system for oxygen, carbon dioxide, and pH measurements in seawater with integrated battery and logger. *Limnol Oceanogr. Methods* 16, 459–473. <https://doi.org/10.1002/lom3.10260>.
- Vera-Vives, A., Perin, G., Morosinotto, T., 2022. High-resolution Photosynthesis-Irradiance Curves in Microalgae. <https://doi.org/10.26124/BEC:2022-0019>.
- Vonshak, A., Novoplansky, N., Silva Benavides, A.M., Torzillo, G., Beardall, J., Palacios, Y.M., 2020. Photosynthetic characterization of two *Nannochloropsis* species and its relevance to outdoor cultivation. *J. Appl. Phycol.* 32, 909–922. <https://doi.org/10.1007/s10811-019-01985-5>.
- Wellburn, A.R., 1994. The spectral determination of chlorophylls a and b, as well as total carotenoids, using various solvents with spectrophotometers of different resolution. *J. Plant Physiol.* 144, 307–313.
- Went, N., Di Marcello, M., Gnaiger, E., 2021. Oxygen Dependence of Photosynthesis and Light-Enhanced Dark Respiration Studied by High-Resolution PhotoRespirometry. <https://doi.org/10.26124/mitofit:2021-0005>.
- Weyer, K.M., Bush, D.R., Darzins, A., Willson, B.D., 2010. Theoretical maximum algal oil production. *Bioenerg. Res.* 3, 204–213. <https://doi.org/10.1007/s12155-009-9046-x>.
- Ye, Z.P., 2007. A new model for relationship between irradiance and the rate of photosynthesis in *Oryza sativa*. *Photosynthetica* 45, 637–640. <https://doi.org/10.1007/s11099-007-0110-5>.
- Zhu, X.-G., Long, S.P., Ort, D.R., 2008. What is the maximum efficiency with which photosynthesis can convert solar energy into biomass? *Curr. Opin. Biotechnol.* 19, 153–159. <https://doi.org/10.1016/j.copbio.2008.02.004>.